Available online at www.sciencedirect.com
SCIENCE DIRECT®
Chemical Physics Letters 407 (2005) 129–134
CHEMICAL PHYSICS LETTERS
www.elsevier.com/locate/cplett

Relaxation of vibrational energy in fullerene suspensions

Scott T. Huxtable [a,*], David G. Cahill [a], Sergei Shenogin [b], Pawel Keblinski [b]

[a] Department of Materials Science and Engineering and the Frederick Seitz Materials Research Laboratory, University of Illinois at Urbana–Champaign, Urbana, IL 61801, United States
[b] Department of Materials Science and Engineering, Rensselaer Polytechnic Institute, Troy, NY 12180, United States

Received 9 March 2004; in final form 3 March 2005
Available online 7 April 2005

Abstract

Picosecond transient absorption is used to measure the thermal decay time of a mixture of higher-order fullerenes suspended in chloroform, toluene, and carbon disulfide. The relaxation time is ≈40 ps, which translates into a small effective interface conductance, $G \approx 14\ \mathrm{MW\ m^{-2}\ K^{-1}}$. Molecular dynamics simulations of a fullerene molecule suspended in octane agree with experiment ($G \approx 10\ \mathrm{MW\ m^{-2}\ K^{-1}}$) and support the conclusion that the 40 ps decay time results from the relaxation of vibrational energy and not the relaxation of electronic excitations.

The relaxation of photo-excited fullerene molecules has been the subject of considerable research in recent years. Time-resolved pump–probe optical measurements have been performed on C_{60} thin films [1–5] and toluene suspensions of C_{60} [6–10], C_{70} [6], and C_{76} and C_{84} [11]. Relaxation times on the order of 40 ps have been observed in many of these experiments [1–4,6,11] and, while all of the authors have attributed the relaxation to a decay or transport property of the electronic system, the authors disagree on the underlying mechanism.

We measured the near-infrared transient absorption of a mixture of higher-order fullerenes suspended in toluene, chloroform, and carbon disulfide and argue that the time-evolution of the optical absorption is a signature of the vibrational relaxation of fullerene molecules, not the decay of electronic excited states. Our speculation that the origin of the relaxation is vibrational is supported by our classical molecular dynamics simulations that do not include electronic effects, yet give a relaxation time comparable to the experimentally measured value. The relaxation of vibrational modes of small molecules in condensed phases has been the subject of research for at least 30 years [12–21]. The relaxation of photo-excited fullerenes provides a useful bridge between the extensive literature on vibrational energy transport in small molecules and more recent studies of interfacial heat transport in nanoparticle [22] and nanotube suspensions [23].

We believe that there are two components to the observed decay. The absorption of a photon excites high frequency vibrational modes within the fullerene which do not couple efficiently with the surrounding fluid. Therefore, the energy associated with these high frequency modes must first be transferred into low frequency vibrational modes before the energy can finally be transmitted to the solvent. Since the entire energy transfer process includes both the cascade of vibrational energy within the fullerene as well as the energy transfer across the interface to the surrounding liquid, the decay is not solely a property of the interface. In fact, we will later argue that the cascade of energy from high frequency modes to low frequency modes may be the

* Corresponding author. Present address: Department of Mechanical Engineering, Virginia Polytechnic Institute and State University, 114-U Randolph Hall, Blacksburg, VA 24061, United States. Fax: +1 540 231 9100.
E-mail address: huxtable@vt.edu (S.T. Huxtable).

0009-2614/$ - see front matter © 2005 Elsevier B.V. All rights reserved.
doi:10.1016/j.cplett.2005.03.052

controlling factor. However, we describe the transfer of energy from the fullerene molecules to the surrounding liquid in terms of an effective interface conductance G as a way of quantifying the entire heat transport process.

Fullerene samples are obtained from the MER Corporation and consist primarily of C_{84}, C_{78}, and C_{76}. The optical density of the fullerene mixture suspended in toluene is shown in Fig. 1. Unlike carbon nanotubes, fullerenes are soluble in toluene, chloroform, and carbon disulfide and do not require the use of a surfactant.

The optical absorption of the higher-order fullerenes near 800 nm is strong [11,24] and, even though the feature in the absorption spectrum near 780 nm is weak, this structure significantly enhances the transient absorption signal. This allows us to achieve high signal-to-noise at the fundamental frequency of the Ti:Sapphire oscillator while using low laser power in order to eliminate concerns of sample degradation.

The experiments are conducted using a modulated laser system [25–27] that is modified for transient-absorption measurements [22]. Sub-picosecond pulses from a Ti:Sapphire mode-locked laser ($740 < \lambda < 800$ nm) are split into a 'pump' beam and a 'probe' beam; the optical path length of the pump beam is adjusted with a mechanical delay stage allowing for time-domain measurements. A small fraction (<1%) of the fullerenes in the beam-path are excited when they absorb an incident photon from the pump beam. The subsequent change in optical absorption of the suspension is then measured with the probe beam. The pump and probe beam powers are each ≈5 mW and the diameters of the laser beams in the sample are 16 μm; thus, the peak laser fluence is ≈60 μJ cm^{-2}.

Unlike some other pump–probe experiments, our measurements do not require that the probe power be smaller than the pump power. Since our signal is given by the product of the pump and probe powers, the steady-state heating of the sample is minimized by setting the pump and probe powers to the same value. The energy density of each optical pulse is small and therefore the transient absorption signal arises from the small fraction of fullerene molecules that absorb a single photon from each pump and probe pulse. Changing the relative pump and probe powers does not change this situation.

For sufficiently small particles, heat transfer between a solid and liquid is controlled by the interface thermal conductance [22]. In other words, the interface is the rate-limiting step for heat transport, not the diffusion of heat in the surrounding fluid, and the thermal decay is an exponential function of time. The decay of the optical absorption of the fullerene suspensions is nearly identical in all three solvents as shown in Fig. 2. For

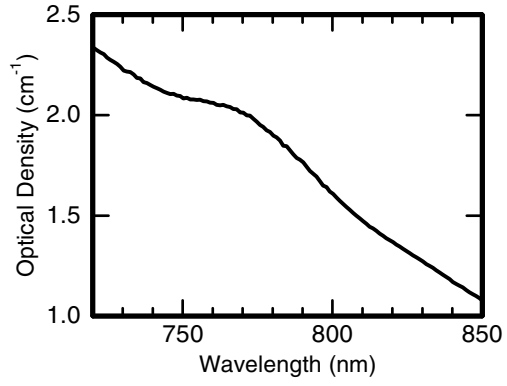

Fig. 1. Optical density of higher-order fullerenes (C_{84}, C_{78}, and C_{76}) suspended in toluene at a concentration of $\approx 1 \times 10^{-3}$ M. The optical path length is 1 cm.

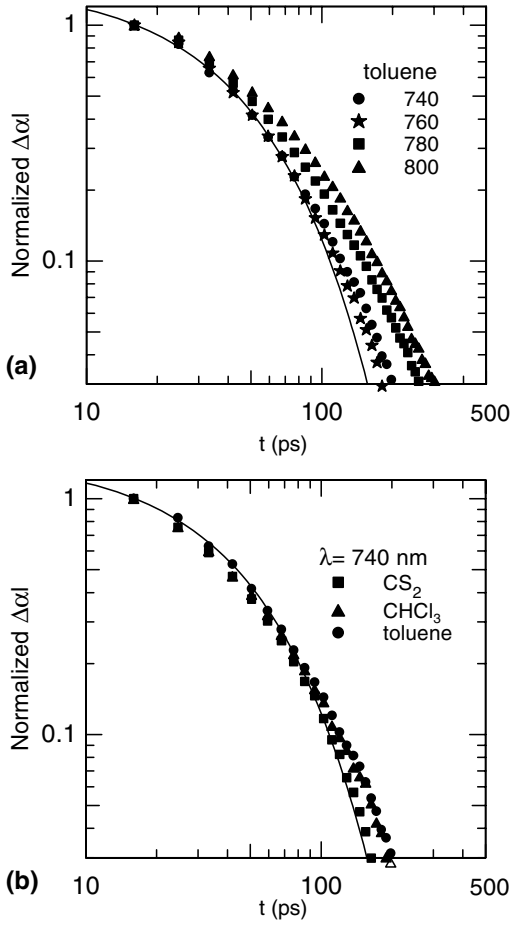

Fig. 2. Transient changes in optical absorption for suspensions of higher-order fullerenes. In (a), the fullerenes are suspended in toluene and the label on each data set refers to the wavelength of the laser (in nm) used for the measurement. For (b), $\lambda = 740$ nm and the label on each data set refers to the solvent used to suspend the fullerenes. The solid lines are single exponential decays with a time constant of $\tau = 40$ ps. α is the absorption coefficient and l is the path length (200 μm). The concentrations are 1 mM in toluene and CS_2 and 0.5 mM in $CHCl_3$. Typical values for $\Delta\alpha l$ were between −8 and −30 ppm at a delay time of $t = 15$ ps.

λ = 740 and 760 nm, the decay is close to single exponential with a time-constant of approximately 40 ps. As the laser wavelength increases to 780 and 800 nm, the decay develops a small-amplitude, long-time tail. We do not fully understand the reason for this slow component to the decay at longer wavelengths, but we suspect this wavelength dependence reflects differences in the sensitivity of our experiment to the decay of electronic excitations.

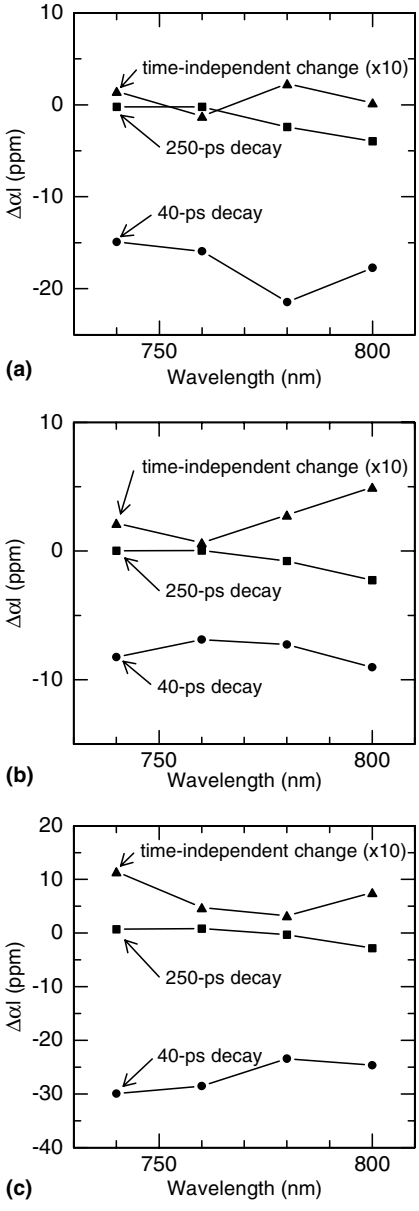

Fig. 3. Amplitudes of the 40 and 250 ps decays in toluene (a), chloroform (b), and carbon disulfide (c). At λ = 740 and 760 nm, the data are nearly single exponential and the amplitude of the 250 ps decay is ≈0. For λ = 780 and 800 nm, the data have a longer decay and the amplitude of the 250 ps time-constant increases. The data also contain a weak time-independent change in optical absorption; these data are multiplied by a factor of 10 for clarity.

The data are fit with a two time-constant exponential at each wavelength with τ_1 = 40 ps and τ_2 = 250 ps. The amplitudes of each time-constant are plotted in Fig. 3 along with the strength of the time-independent change in absorption. The long-time tail of the decay observed at longer wavelengths appears as an increase in amplitude of the τ_2 relaxation.

One issue that warrants discussion is the possibility that some of the fullerene molecules form aggregates in solution [28,29]. Cho et al. [11] found that aggregation of C_{84} molecules in toluene becomes significant at concentrations on the order of 0.1 mM, while the concentrations of the suspensions we used were 0.5 mM in chloroform and 1 mM in toluene and carbon disulfide. To address this issue, we prepared separate suspensions in chloroform (0.5 mM) and toluene (1 mM) and measured the optical density of each sample. The two suspensions were then spun in a centrifuge at 9000*g* for 3 h and the optical density of each supernatant was then measured. We found that the optical density of the supernatant was identical to the optical density of the original sample for both solvents indicating that there were no large (>20 nm) aggregates present in the original solutions.

The effective interface thermal conductance G is determined using [23]

$$G = \frac{C}{A\tau}, \tag{1}$$

where C is the fullerene heat capacity, A is the fullerene surface area, and τ is the time constant of the thermal decay. The measured heat capacity for C_{60} at room temperature [30] is essentially identical to that of graphite [31] with $C \approx 0.75$ J g^{-1} K^{-1}. The heat capacity per unit area for the fullerene should be identical to the heat capacity per unit area of an atomic layer of graphite, 5.6×10^{-4} J m^{-2} K^{-1}. Note that this value is equivalent to the heat capacity per unit area obtained by using a mean diameter of 7.16 Å to calculate the surface area of the fullerene. Using 40 ps for the time constant of the thermal decay and 5.6×10^{-4} J m^{-2} K^{-1} for the heat capacity per unit area for the surface of the fullerene, we find $G \approx 14$ MW m^{-2} K^{-1}.

To gain a more detailed understanding of the relaxation process, we performed classical molecular dynamics simulations of the thermal relaxation of a C_{84} molecule suspended in a hydrocarbon liquid. For the sake of comparison with our recent simulations of carbon nanotube suspensions [23], we select octane as a model hydrocarbon liquid. In all reported simulations, we immerse a C_{84} molecule in a melt of 228 octane molecules (6012 explicit atoms). Both carbon and hydrogen atoms are modeled explicitly and periodic boundary conditions are applied in all directions. Interatomic interactions are calculated using a PCFF force-field [32,33] with the additional second-order cross terms in the potential

energy expression. The pressure and temperature are set to 1 atm and 298 K, respectively. Under these conditions, the density of the octane melt in all models is equal to 0.71 g cm^{-3}, which is close to the measured density of octane ($\rho = 0.7025$ g cm^{-3}).

To mimic the experiment, after equilibrating the system at 1 atm and 298 K, we heat the fullerene instantaneously to 500 K by rescaling the velocities of carbon atoms in the C_{84} molecule, and the system is then allowed to relax without a thermostat at constant energy. Equilibration of the fullerene molecule occurs on a time scale of only a few picoseconds while the time scale for the cooling of the molecule in the simulation is ≈150 ps.

Fig. 4 shows the average temperatures of the C_{84} molecule and octane liquid as a function of time. Since the total heat capacity of the liquid is much larger than that of C_{84}, the liquid temperature is almost constant, while the temperature of the fullerene molecule decreases to equilibrate with the liquid. We observe an exponential relaxation with a time constant of ≈150 ps, which is almost 4 times larger than the decay obtained in the experiment. However, the lack of quantization of the high frequency modes in the classical molecular dynamics simulations results in a heat capacity for the simulated fullerene that is factor of 2.8 greater than the experimentally measured fullerene heat capacity. Thus, from Eq. (1), the 150 ps decay in the simulation corresponds to an interface conductance of $G \approx 10\ \mathrm{MW\,m^{-2}\,K^{-1}}$, which is comparable to the experimental value of $G \approx 14\ \mathrm{MW\,m^{-2}\,K^{-1}}$. Since these molecular dynamics simulations do not include electronic effects, yet are in reasonable agreement our experimental results, we propose that our measured 40 ps decay – and the 30–60 ps decay time observed in much of the literature [1–4,6,11] – is a signature of the relaxation of vibrational energy rather than the relaxation of electronic excitations.

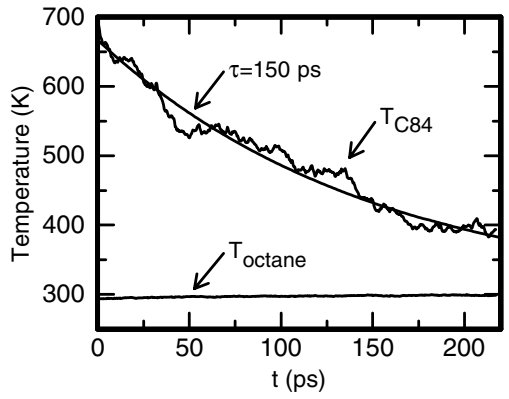

Fig. 4. Thermal decay of a C_{84} molecule in octane determined from the molecular dynamics simulation. The simulation does not account for the quantization of the high frequency modes in the fullerene, thus the heat capacity of the fullerene in the simulation is a factor of 2.8 times larger than the experimentally measured value. Accounting for this difference in heat capacity, the decay of ≈150 ps in the simulation corresponds to $G \approx 10\ \mathrm{MW\,m^{-2}\,K^{-1}}$, which is equivalent to an experimental decay of ≈54 ps.

This patching scheme we apply by normalizing the relaxation time by the heat capacity relies mainly on the assumption that the high frequency modes present in the classical system do not significantly affect energy flow between the fullerene and the liquid. This is a reasonable assumption considering that only soft forces with associated low frequencies act between the fullerenes and the liquid. While our molecular dynamics simulations naturally lack many detailed features of the real system, some critical parameters of these studies compare well with the experiment. For example, the vibrational spectra of the fullerenes are well reproduced, and the magnitude of the non-bonded interactions responsible for energy transfer between the fullerene and the organic liquid is well captured.

The molecular dynamics simulations also provide further insight into the overall mechanisms for vibrational energy transfer from the fullerenes to the liquid. The simulations indicate that the low frequency vibrational modes of the fullerene are close to the temperature of the liquid while the high frequency modes, which contain most of the heat capacity of the fullerene molecule, are in equilibrium with each other at a higher temperature. Thus, the limiting step for the flow of vibrational energy appears to be the cascade of energy from the large number of high frequency modes into the small number of low frequency modes within the fullerene that couple with the surrounding liquid.

It is interesting to compare the values of interface conductance obtained in this work to those measured for a carbon nanotube–surfactant interface [23], $G \approx 12\ \mathrm{MW\,m^{-2}\,K^{-1}}$, and simulated for a nanotube–octane liquid interface [23], $G \approx 25\ \mathrm{MW\,m^{-2}\,K^{-1}}$. The experimentally measured decays of fullerenes and nanotubes are similar, whereas in simulations the conductance of the C_{84}–octane interface is a factor of two smaller than that of the corresponding nanotube–octane interface.

The lower thermal conductance of the C_{84}–liquid interface obtained in simulations can be explained as follows. Both fullerenes and carbon nanotubes only interact with the surrounding liquid through weak van der Waals interactions. Therefore, strong coupling across the solid–liquid interface is possible only via low frequency modes [23]. Carbon nanotubes possess low frequency modes in the form of bending and squeezing oscillations, however, these low frequency modes are not as abundant in fullerenes due to the geometry and smaller size of the fullerene molecule.

To illustrate the above discussion more clearly, we show the vibrational density of states (DOS) for an octane liquid along with C_{84} molecules in Fig. 5. The DOS is obtained from the Fourier transform of the atomic

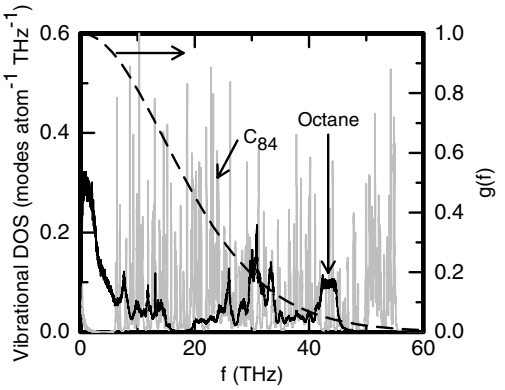

Fig. 5. Vibrational density of states (DOS) for a fullerene molecule and liquid octane. Octane also has a small peak at 90 THz due to the C–H stretch. The dashed line corresponds to the right hand axis where $g(f)$ is the heat capacity per mode relative to the equipartition limit. The DOS of octane is large at low frequency; however, the DOS of the fullerene is small in this frequency range. Since there is little direct overlap in the frequency space between low frequency modes in the liquid and C_{84}, there is limited coupling between the solid and liquid. This lack of efficient coupling leads to a low thermal conductance at the C_{84}–octane interface.

velocity autocorrelation function [34]. The DOS for the octane liquid has a number of sharp peaks at high frequencies representing intramolecular vibrations of covalently bonded carbon and hydrogen atoms and a low frequency peak with a shoulder that extends to about 5 THz. This low frequency peak is associated with weak dispersion forces between octane molecules. Therefore, thermal coupling between the liquid and the fullerene is expected to occur via soft phonons with frequencies falling within the first DOS peak for the liquid. However, the DOS of the fullerene is exceedingly small under the first peak of the liquid DOS. The only exception is a small peak near zero frequency that is associated with the C_{84} center of mass motion. Therefore, except for the center of mass motion, there is little direct overlap in the frequency space between low frequency modes in the liquid and C_{84}. This leads to a low thermal conductance at the C_{84}–octane interface. By contrast, carbon nanotubes have a number of low frequency modes associated with tube bending and squeezing that couple well with the liquid and lead to a higher interface conductance [23].

If the above reasoning is correct in explaining the factor of two difference between the conductance values from the simulations of the nanotube–octane and fullerene–octane interfaces, the question then becomes, 'Why do we not see this difference in the experiments?' One possible explanation of this discrepancy is that the carbon nanotubes may have been bundled to some extent in the experiment resulting in a longer relaxation time and lower conductance with respect to the isolated nanotubes used in simulations. Another difference is that the conversion of a single photon into thermal energy results in a temperature rise of ≈200 K for a fullerene molecule due to its small heat capacity, while the temperature rise in our experiments on carbon nanotubes is on the order of only a few degrees Kelvin. Therefore, the measured decay time for the fullerenes would then depend on whether the heat capacity or the effective interface conductance increases with temperature more rapidly.[1]

Finally, we show that an analysis of the vibrational cooling of a thoroughly studied polyatomic molecule, azulene, gives comparable values for the effective thermal conductance of the interface between the azulene molecule and solvents. Sukowski et al. [15] found vibrational cooling times between 15 and 40 ps for azulene depending on the solvent. We can estimate G from these decay times using Eq. (1) with additional knowledge of the heat capacity and surface area of the azulene molecule. The heat capacity is found in the literature to be 1.9 J g^{-1} K^{-1} [35], or 4×10^{-22} J K^{-1} for a single molecule. Determining the surface area is not as straightforward, but we can make a crude estimate by assuming that the area per carbon atom in azulene is twice the area per carbon atom in a fullerene molecule (with the factor of two arising from the fact that the solvent is present on both sides of an azulene molecule rather than just on the outside of a fullerene molecule). Using this approach, the surface area of an azulene molecule is 5.4×10^{-19} m^2. This gives $G = 19$ MW m^{-2} K^{-1} for $\tau = 40$ ps and $G = 50$ MW m^{-2} K^{-1} for $\tau = 15$ ps. These values are comparable to the interface conductance measured for the fullerenes with the major difference being that azulene exhibits a dependence on the solvent while the fullerenes do not. The structure of azulene, a seven-member ring fused to a five-member ring, may make the molecule softer with respect to bending. Thus, it may couple more efficiently with specific liquids leading to the larger interface conductance values.

In this Letter, we reported experimental studies and molecular-level simulations of vibrational relaxation of optically excited fullerene solutions. Considering the reasonable agreement between the experiment and the simulations and the fact that the molecular dynamics simulations do not include electronic effects, our combined results suggest that the observed changes in transient absorption may be the result vibrational energy relaxation rather than the decay of electronic excitations.

[1] We note that the decays observed for thin fullerene films [1–4] may also be the result of thermal relaxation. Since only a fraction of the fullerene molecules in a solid film absorb energy from a laser pulse, the excited fullerene molecules will cool by transferring energy to neighboring molecules much like the fullerenes in solution lose heat to the surrounding liquid.

Acknowledgments

We thank Zhenbin Ge for carrying out the centrifuge experiments. This work was supported by DOE Grant No. DEFG02-01ER45938. Sample characterization used the facilities of the Center for Microanalysis of Materials, which is partially supported by the US Department of Energy under Grant No. DEFG02-91-ER45439. Optical measurements were performed in the Laser Facility of the Seitz Materials Research Laboratory. Work of P.K. and S.S. was supported by DOE Grant No. DE-FG02-04ER46104, and a grant from Phillip Morris, USA.

References

[1] R.A. Cheville, N.J. Halas, Phys. Rev. B 45 (1992) 4548.
[2] S.B. Fleischer, E.P. Ippen, G. Dresselhaus, M.S. Dresselhaus, A.M. Rao, P. Zhou, P.C. Eklund, Appl. Phys. Lett. 62 (1993) 3241.
[3] V.M. Farztdinov, Y.E. Lozovik, Y.A. Matveets, A.G. Stepanov, V.S. Letokhov, J. Phys. Chem. 98 (1994) 3290.
[4] S. Ishihara, I. Ikemoto, S. Suzuki, K. Kikuchi, Y. Achiba, T. Kobayashi, Chem. Phys. Lett. 295 (1998) 475.
[5] T. Juhasz, X.H. Hu, C. Suarez, W.E. Bron, E. Maiken, P. Taborek, Phys. Rev. B 48 (1993) 4929.
[6] M.R. Wasielewski, M.P. O'Neil, K.R. Lykke, M.J. Pellin, D.M. Gruen, J. Am. Chem. Soc. 113 (1991) 2774.
[7] V. Klimov, L. Smilowitz, H. Wang, M. Grigorova, J.M. Robinson, A. Koskelo, B.R. Mattes, F. Wudl, D.W. McBranch, Res. Chem. Intermed. 23 (1997) 587.
[8] R.J. Sension, C.M. Phillips, A.Z. Szarka, W.J. Romanow, A.R. McGhie, J.P. McCauley, A.B. Smith, R.M. Hochstrasser, J. Phys. Chem. 95 (1991) 6075.
[9] T.W. Ebbesen, K. Tanigaki, S. Kuroshima, Chem. Phys. Lett. 181 (1991) 501.
[10] A.G. Stepanov, M.T. Portella-Oberli, A. Sassara, M. Chergui, Chem. Phys. Lett. 358 (2002) 516.
[11] H.S. Cho, T.K. Ahn, S.I. Yang, S.M. Jin, D. Kim, S.K. Kim, H.D. Kim, Chem. Phys. Lett. 375 (2002) 292.
[12] A. Laubereau, D. von der Linde, W. Kaiser, Phys. Rev. Lett. 28 (1972) 1162.
[13] A. Seilmeier, J.P. Maier, F. Wondrazek, W. Kaiser, J. Phys. Chem. 90 (1986) 104.
[14] H. Kim, D.D. Dlott, J. Chem. Phys. 94 (1991) 8203.
[15] U. Sukowski, A. Seilmeier, T. Elsaesser, S.F. Fischer, J. Chem. Phys. 93 (1990) 4094.
[16] D. Schwarzer, C. Hanisch, P. Kutne, J. Troe, J. Phys. Chem. A 106 (2002) 8019.
[17] S.A. Kovalenko, R. Schanz, H. Hennig, N.P. Ernsting, J. Chem. Phys. 115 (2001) 3256.
[18] T. Okazaki, N. Hirota, T. Nagata, A. Osuka, M. Terazima, J. Phys. Chem. A 103 (1999) 9591.
[19] T. Elsaesser, W. Kaiser, Annu. Rev. Phys. Chem. 42 (1991) 83.
[20] G. Seifert, T. Patzlaff, H. Graener, Phys. Rev. Lett. 88 (2002) 1474021.
[21] J.C. Deàk, Y. Pang, T.D. Sechler, Z. Wang, D.D. Dlott, Science 306 (2004) 473.
[22] O.M. Wilson, X. Hu, D.G. Cahill, P.V. Braun, Phys. Rev. B 66 (2002) 224301-1.
[23] S.T. Huxtable, D.G. Cahill, S. Shenogin, L. Xue, R. Ozisik, P. Barone, M. Usrey, M.S. Strano, G. Siddons, M. Shim, P. Keblinski, Nat. Mater. 2 (2003) 731.
[24] E. Koudoumas, M. Konstantaki, A. Mavromanolakis, X. Michaut, S. Couris, S. Leach, J. Phys. B 34 (2001) 4996.
[25] D.G. Cahill, K. Goodson, A. Majumdar, J. Heat Transfer 124 (2002) 223.
[26] R.M. Costescu, M.A. Wall, D.G. Cahill, Phys. Rev. B 67 (2003) 54302-1.
[27] K.E. O'Hara, X. Hu, D.G. Cahill, J. Appl. Phys. 90 (2001) 4852.
[28] H.N. Ghosh, A.V. Sapre, J.P. Mittal, J. Phys. Chem. 100 (1996) 9439.
[29] S. Nath, H. Pal, D.K. Palit, A.V. Sapre, J.P. Mittal, J. Phys. Chem. 102 (1998) 10158.
[30] T. Matsuo, H. Suga, W.I.F. David, R.M. Ibberson, P. Bernier, A. Zahab, C. Fabre, A. Rassat, A. Dwokin, Solid State Commun. 83 (1992) 711.
[31] Y.S. Touloukian, Thermophysical Properties of Matter, IFI/Plenum Press, New York, 1979.
[32] Discover®, Forcefield Simulation User Guide, Molecular Simulations Inc., San Diego, 1996.
[33] H. Sun, S.J. Mumby, J.R. Maple, A.T. Hagler, J. Am. Chem. Soc. 116 (1994) 2978.
[34] M.P. Allen, D.J. Tildesley, Computer Simulation of Liquids, Oxford University Press, New York, 1987.
[35] C.L. Yaws, Chemical Properties Handbook, McGraw-Hill, New York, 1999.